Electrically driven green, olivine, and amber color nanopyramid light emitting diodes

Shih-Pang Chang,[1] Jet-Rung Chang,[3] Kuok-Pan Sou,[1] Mei-Chun Liu,[2] Yuh-Jen Cheng,[1,2,*] Hao-Chung Kuo,[1,4] and Chun-Yen Chang[3]

[1]*Department of Photonics, National Chiao Tung University, 1001 Ta Hsueh Rd. Hsinchu 300, Taiwan*
[2]*Research Center for Applied Sciences, Academia Sinica, 128 Sec. 2, Academia Rd, Nankang, Taipei 115, Taiwan*
[3]*Department of Electronic Engineering, National Chiao Tung University, 1001 Ta Hsueh Rd., Hsinchu 300, Taiwan*
[4]*hckuo@faculty.nctu.edu.tw*
[*]*yjcheng@sinica.edu.tw*

Abstract: We report the fabrication and studies of electrically driven green, olivine, and amber color nanopyramid GaN light emitting diodes (LEDs). InGaN/GaN multiple quantum wells (MQWs) were grown on the nanopyramid semipolar facets. Compared with the commonly used (0001) c-plane MQWs, the semipolar facet has lower piezoelectric field, resulting in much faster radiative recombination efficiency. This is important for high In content MQWs. The measured internal quantum efficiencies for green, olivine, and amber color LED are 30%, 25%, and 21%, respectively. The radiative and non-radiative lifetime of the semipolar MQWs are also investigated.

OCIS codes: (250.0250) Optoelectronics; (160.6000) Semiconductor materials.

References and links

1. J. Wu, W. Walukiewicz, K. Yu, J. Ager, E. Haller, H. Lu, and W. Schaff, "Small band gap bowing in $In_{1-x}Ga_xN$ alloys," Appl. Phys. Lett. **80**(25), 4741–4743 (2002).
2. P. T. Barletta, E. A. Berkman, B. F. Moody, N. A. El-Masry, A. M. Emara, M. J. Reed, and S. M. Bedair, "Development of green, yellow, and amber light emitting diodes using InGaN multiple quantum well structures," Appl. Phys. Lett. **90**(15), 151109 (2007).
3. D. Fuhrmann, C. Netzel, U. Rossow, A. Hangleiter, G. Ade, and P. Hinze, "Optimization scheme for the quantum efficiency of GaInN-based green-light-emitting diodes," Appl. Phys. Lett. **88**(7), 071105 (2006).
4. Y.-L. Lai, C.-P. Liu, Y.-H. Lin, R.-M. Lin, D.-Y. Lyu, Z.-X. Peng, and T.-Y. Lin, "Effects of the material polarity on the green emission properties of InGaN/GaN multiple quantum wells," Appl. Phys. Lett. **89**(15), 151906 (2006).
5. F. Bernardini, V. Fiorentini, and D. Vanderbilt, "Spontaneous polarization and piezoelectric constants of III-V nitrides," Phys. Rev. B **56**(16), R10024–R10027 (1997).
6. N. Akopian, G. Bahir, D. Gershoni, M. D. Craven, J. S. Speck, and S. P. DenBaars, "Optical evidence for lack of polarization in (11-20) oriented GaN/(AlGa)N quantum structures," Appl. Phys. Lett. **86**(20), 202104 (2005).
7. M. Ueda, K. Kojima, M. Funato, Y. Kawakami, Y. Narukawa, and T. Mukai, "Epitaxial growth and optical properties of semipolar (11-22) GaN and InGaN/GaN quantum wells on GaN bulk substrates," Appl. Phys. Lett. **89**(21), 211907 (2006).
8. R. Sharma, P. M. Pattison, H. Masui, R. M. Farrell, T. J. Baker, B. A. Haskell, F. Wu, S. P. DenBaars, J. S. Speck, and S. Nakamura, "Demonstration of a semipolar (10-1-3) InGaN/GaN green light emitting diode," Appl. Phys. Lett. **87**(23), 231110 (2005).
9. K. Hiramatsu, "Epitaxial lateral overgrowth techniques used in group III nitride epitaxy," J. Phys. Condens. Matter **13**(32), 6961–6975 (2001).
10. C. Liu, A. Satka, L. K. Jagadamma, P. R. Edwards, D. Allsopp, R. W. Martin, P. Shields, J. Kovac, F. Uherek, and W. Wang, "Light emission from InGaN quantum wells grown on the facets of closely spaced GaN nano-pyramids formed by nano-imprinting," Appl. Phys. Express **2**(12), 121002 (2009).
11. I. H. Wildeson, R. Colby, D. A. Ewoldt, Z. Liang, D. N. Zakharov, N. J. Zaluzec, R. E. García, E. A. Stach, and T. D. Sands, "III-nitride nanopyramid light emitting diodes grown by organometallic vapor phase epitaxy," J. Appl. Phys. **108**(4), 044303 (2010).
12. T. Kim, J. Kim, M.-S. Yang, S. Lee, Y. Park, U.-I. Chung, and Y. Cho, "Highly efficient yellow photoluminescence from {11–22} InGaN multiquantum-well grown on nanoscale pyramid structure," Appl. Phys. Lett. **97**(24), 241111 (2010).
13. H. Yu, L. K. Lee, T. Jung, and P. C. Ku, "Photoluminescence study of semipolar {10-11} InGaN/GaN multiple quantum wells grown by selective area epitaxy," Appl. Phys. Lett. **90**(14), 141906 (2007).

#191394 - $15.00 USD Received 29 May 2013; revised 23 Aug 2013; accepted 12 Sep 2013; published 23 Sep 2013

14. Y.-H. Ko, J.-H. Kim, L.-H. Jin, S.-M. Ko, B.-J. Kwon, J. Kim, T. Kim, and Y.-H. Cho, "Electrically driven quantum dot/wire/well hybrid light-emitting diodes," Adv. Mater. **23**(45), 5364–5369 (2011).
15. Y. Kawakami, K. Omae, A. Kaneta, K. Okamoto, Y. Narukawa, T. Mukai, and S. Fujita, "In inhomogeneity and emission characteristics of InGaN," J. Phys. Condens. Matter **13**(32), 6993–7010 (2001).
16. Y.-H. Cho, G. H. Gainer, A. J. Fischer, J. J. Song, S. Keller, U. K. Mishra, and S. P. DenBaars, "S-shaped temperature-dependent emission shift and carrier dynamics in InGaN/GaN multiple quantum wells," Appl. Phys. Lett. **73**(10), 1370–1372 (1998).
17. H. P. D. Schenk, M. Leroux, and P. de Mierry, "Luminescence and absorption in InGaN epitaxial layers and the van Roosbroeck–Shockley relation," J. Appl. Phys. **88**(3), 1525–1534 (2000).
18. A. Bell, S. Srinivasan, C. Plumlee, H. Omiya, F. A. Ponce, J. Christen, S. Tanaka, A. Fujioka, and Y. Nakagawa, "Exciton freeze-out and thermally activated relaxation at local potential fluctuations in thick $Al_xGa_{1-x}N$ layers," J. Appl. Phys. **95**(9), 4670–4674 (2004).
19. Y. Narukawa, S. Saijou, Y. Kawakami, S. Fujita, T. Mukai, and S. Nakamura, "Radiative and nonradiative recombination processes in ultraviolet light-emitting diode composed of an $In_{0.02}Ga_{0.98}N$ active layer," Appl. Phys. Lett. **74**(4), 558–560 (1999).
20. T. Li, A. M. Fischer, Q. Y. Wei, F. A. Ponce, T. Detchprohm, and C. Wetzel, "Carrier localization and nonradiative recombination in yellow emitting InGaN quantum wells," Appl. Phys. Lett. **96**(3), 031906 (2010).
21. P. G. Eliseev, P. Perlin, J. Lee, and M. Osinski, "Blue temperature-induced shift and band-tail emission in InGaN-based light sources," Appl. Phys. Lett. **71**(5), 569–571 (1997).
22. Y. Narukawa, Y. Kawakami, S. Fujita, and S. Nakamura, "Dimensionality of excitons in laser-diode structures composed of $In_xGa_{1-x}N$ multiple quantum wells," Phys. Rev. B **59**(15), 10283–10288 (1999).
23. S.-P. Chang, Y.-C. Chen, J.-K. Huang, Y.-J. Cheng, J.-R. Chang, K.-P. Sou, Y.-T. Kang, H.-C. Yang, T.-C. Hsu, H.-C. Kuo, and C.-Y. Chang, "Electrically driven nanopyramid green light emitting diode," Appl. Phys. Lett. **100**(6), 061106 (2012).
24. N. K. van der Laak, R. A. Oliver, M. J. Kappers, and C. J. Humphreys, "Role of gross well-width fluctuations in bright, green-emitting single InGaN/GaN quantum well structures," Appl. Phys. Lett. **90**(12), 121911 (2007).
25. A. Hangleiter, F. Hitzel, C. Netzel, D. Fuhrmann, U. Rossow, G. Ade, and P. Hinze, "Suppression of nonradiative recombination by v-shaped pits in GaInN/GaN quantum wells produces a large increase in the light emission efficiency," Phys. Rev. Lett. **95**(12), 127402 (2005).

1. Introduction

The III-nitride based LED has gained great research interests due to its promising potential in high efficient lighting applications. The band gap of InGaN semiconductor can be potentially varied from UV (3.4 eV) to near infrared (0.7 eV) [1]. In principle, such devices can cover the entire visible spectrum, thereby promising multiple color lighting applications without the use of down-converting phosphors which have significant Stokes shift energy loss. Conventional InGaN/GaN MQWs are often grown on the polar c-plane surface. The typical emission wavelength is in the blue region, where the efficiency is optimal. To have emission wavelength in the green to red region, it is required to increase In incorporation. However, the efficiency drops rapidly as In concentration increases [2,3]. One of the primary causes is the large strain induced piezoelectric field due to the lattice mismatch among the sapphire template, GaN, and InGaN. The piezoelectric field reduces spatial electron-hole wave function overlap and leads to low internal quantum efficiency (IQE) [4,5]. One way to reduce this problem is to grow MQWs on other crystal planes with lower polarization field. Experimental demonstrations have shown improved emission efficiency for MQWs grown on semipolar and nonpolar substrates [6–8]. These substrates are, however, not readily available.

The semipolar and nonpolar crystal surfaces can be found in naturally formed crystalline structure using 3-dimensional epitaxial growth. Nano size hexagonal pyramids can be grown by selective area growth on the opening holes of a SiO2 masked c-plane GaN substrate, which is more readily available [9]. The pyramid facets are typically {10-11} or {11-22} semipolar planes. In addition to the low polarization field of these crystal planes, the small footprint of 3D nano structure on a substrate can also provide better strain relaxation, resulting in lower defect density and the further reduction of the piezoelectric field. There have been strong interests in using these semipolar pyramid facets for LED applications, in particular high In content LEDs [10,11]. Photoluminescent (PL) studies of these nano scale facets have demonstrated significant reduction in the polarization field and better IQE [12,13]. The reduced polarization field leads to much faster radiative recombination lifetime. The IQE is however not enhanced in proportional magnitude. The reason lies in the fact that the non-radiative lifetime of semipolar InGaN QWs is also shorten, which has not been well

#191394 - $15.00 USD Received 29 May 2013; revised 23 Aug 2013; accepted 12 Sep 2013; published 23 Sep 2013

investigated. Reports for the electrical injection of high In content nanopyramid LED are also very limited [14].

Here, we report the fabrication and properties of electrically driven nanopyramid LEDs. High In content MQWs intended for green, olivine, and amber colors are fabricated. A thin p-GaN layer conformal to the nanopyramid geometry was grown on the nanopyramid facets. The time-resolved photoluminescence (TRPL) measurement shows fast sub-ns radiative recombination lifetime. The peak emission wavelengths of these samples monotonically decrease with increasing temperature, indicating less localized potential [15–18] which causes faster non-radiative lifetime. The internal quantum efficiencies (IQEs) of the green, olivine, and amber color LED are 30%, 25%, and 21%, respectively, which are hard to achieve for c-plane MQWs in the same wavelength range. The efficiency decrease is attributed to the increase of piezoelectric field in MQWs as In content increases.

2. Fabrication and characterization

The fabrication steps are shown in Figs. 1(a)-1(d). Nanopillars were first fabricated by patterned top-down etching of an n-doped GaN substrate [Fig. 1(a)]. The nanopillar side walls were coated with spin-on-glass [Fig. 1(b)], followed by a MOCVD regrowth to grow nanopyramids and InGaN/GaN MQWs on the tops of nanopillars [Fig. 1(c)]. The spin-on-glass coating was to prevent GaN from growing on the side walls during the regrowth. A thin layer of p-GaN conformal to the pyramid facets was subsequently grown to form arrays of nanopyramid LEDs. A standard LED fabrication process was used to fabricate LED chips, where indium tin oxide (ITO) was used as a transparent conducting layer [Fig. 1(d)]. Three LEDs with different In concentrations are fabricated. The peak emission wavelengths are 500, 550, and 600 nm. Their visual colors appear to be green, olivine, and amber color, respectively. For the convenience of reference, each is referred as G-, O-, and A-LED. The high resolution tunneling electron microscope (HRTEM) image taken by a JEOL JEM-2100 electron microscope at 200KV is shown in Fig. 1(e), showing the MQWs grown on the inclined pyramid facets. The measured QW and barrier widths are 2 nm and 8 nm, respectively. The widths are uniform due to the crystalline facet growth. The darker color at the bottom pyramid coalescent boundaries implies possible higher In content and/or coalescent defects. There are also some coalescent defects at the apex region.

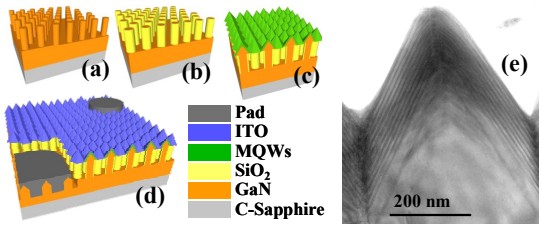

Fig. 1. The fabrication steps of a nanopyramid LED. (a) Nanopillars by patterned top-down etch. (b) Nanopillar sidewall coated with oxide. (c) Nanopyramids grown on the top of nanopillars, followed by MQW growth. (d) Top surface indium tin oxide (ITO) deposition and metal pad fabrication. (e) HRTEM cross-section image taken from a nanopillar sample right after MQW growth.

The photoluminescent properties of the nanopyramids were investigated by spectrally resolved cathodoluminescent (CL) microscopy, as shown in Figs. 2(a)-2(f). The images taken from the G-LED sample are shown here to illustrate the general characteristics. Figure 2(a) is the plane view scanning electron microscope (SEM) image, showing the nanopyramid structure. Figures 2(b)-2(f) are the spectrally resolved CL images taken from 460 to 560 nm at every 20 nm step. The bright pattern indicates the emission location of the selected wavelength on the pyramid facets. The much lower CL intensity in Fig. 2(f) is due to defects in MQWs at the apex region. The dark central triangle pattern becomes smaller as the wavelength is scanned from 480 nm to 560 nm, as shown in Figs. 2(b)-2(f), indicating that it moves up the pyramids as the wavelength increases. The bright triangle ring pattern basically

#191394 - $15.00 USD Received 29 May 2013; revised 23 Aug 2013; accepted 12 Sep 2013; published 23 Sep 2013

follows the pyramid height contour, as can be seen by comparing it with the pyramid SEM image Fig. 2(a). This indicates that the MQW emission redshifts as location moves from the bottom to apex region on the pyramid facets. It is attributed to the increase of In incorporation as the region moves up the facet. The variation of In concentration in MQWs was confirmed by an energy dispersive spectrometer (EDS) Oxford X-Max. The same specimen used for the previous cross section HRTEM analysis was used for the EDS analysis. The e-beam was focused on the InGaN QW and scanned along the QW. The In content increases from 15% to 30% as the QW is scanned from bottom to apex region. There is no noticeable QW thickness variation in the HRTEM image. We therefore attribute this redshift mainly to the In incorporation changes.

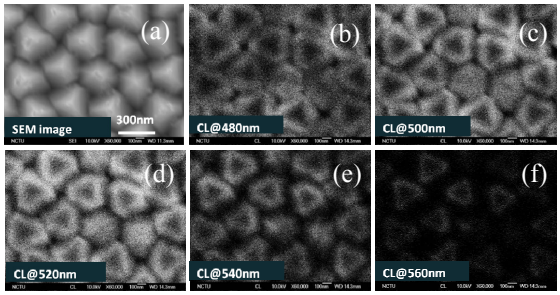

Fig. 2. (a) SEM top view. (b)-(f) Spectrally resolved CL images at various wavelength. The bright pattern follows the pyramid height contour, indicating a redshift of MQW emission as the location moves from the bottom to top of nanopyramids.

3. Discussion

The internal quantum efficiencies (IQE) of these samples were investigated by the temperature dependent PL measurement. Figure 3(a) shows the integrated PL intensity over the emission spectrum versus temperature from 20 to 300 K. The IQE is assumed to be close to unity at low temperature because non-radiative recombination is mostly suppressed at low temperature [19]. The IQE was obtained by normalizing the integrated PL intensity to its low temperature value. The measured room temperature IQEs of G-, O-, and A-LED are 30%, 25%, and 21%, respectively. These values are hard to achieve for c-plane MQWs, e.g. 12% was reported for c-plane MQWs at 570 nm [20]. The decrease in efficiency as the sample changes from G- to A-LED is because the increase of In content induces larger internal polarization field which results in larger electron-hole wave function separation. We have also measured the PL lifetimes by TRPL, as shown in Fig. 3(b). The PL lifetime decreases with increasing temperature as the non-radiative process is thermally activated. The PL emission peak energy versus temperature is shown in Fig. 3(c). The peak energy monotonically decreases with increasing temperature. It is different from the often observed red-blue-red shift (S-curve) in the c-plane MQWs, which is attributed to the localized states due to the fluctuations of In distribution in InGaN MQWs [16,21]. The absence of S-curve implies a significant reduction of localized potentials for MQWs grown on the nanopyramid facets. This could be due to the better strain relaxation provided by the nanostructure and/or the growth property of the pyramid semipolar facets [10,11].

#191394 - $15.00 USD Received 29 May 2013; revised 23 Aug 2013; accepted 12 Sep 2013; published 23 Sep 2013

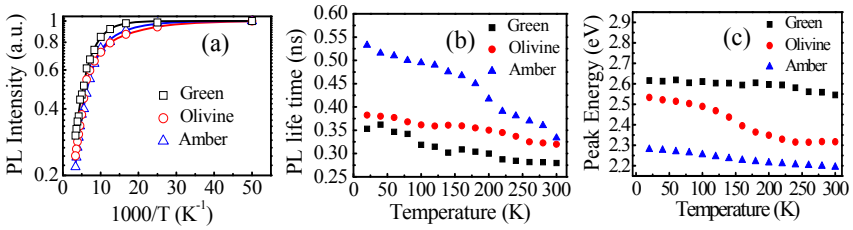

Fig. 3. (a) Integrated PL intensity versus temperature. The PL intensity is normalized to its value at 20K. (b) Time resolved PL decay time constant versus temperature. (c) Emission peak energy versus temperature.

The PL lifetime τ_{PL} is related to the radiative and nonradiative lifetime, τ_r and τ_{nr}, by $1/\tau_{PL} = 1/\tau_r + 1/\tau_{nr}$. The IQE η is defined as $\eta = \tau_{PL}/\tau_r$. From the measured τ_{PL} and η, we can obtain the temperature dependent τ_r and τ_{nr}, as shown in Figs. 4(a)-4(c). The τ_r remains constant at low temperature below ~50 K and increases about linearly at higher temperature. This relates to the well known behavior that the radiative lifetime is nearly constant for a localized exciton and increases linearly with temperature for a 2D confined exciton [22]. The measured result indicates that, at low temperature, the excitons are trapped in localized potentials due to inhomogeneous In composition in MQWs. As temperature increases, excitons are excited out of the traps and become free excitons in the 2D MQWs, resulting in approximately linearly increasing radiative lifetime with temperature. The rather low temperature transition implies small localized potentials. The measured room temperature (τ_r, τ_{nr}) for G-, O-, and A-LED are (0.92, 0.40), (1.3, 0.42), and (1.5, 0.43) ns, respectively. These τ_r values are about two orders of magnitude smaller than the typical hundreds of ns value reported for c-plane MQWs [20,23]. The faster radiative recombination is attributed to the lower polarization field in the nanopyramid facets. It is worth to note that the IQE is not determined by τ_r alone. τ_{nr} also plays an equally important role. The measured τ_{nr} is also significantly shortened as compared with the reported hundred ns lifetime [20]. This is attributed to the above observed less localized potential in semipolar MQWs. The localized potential has been considered as one of the important factors in preventing the capture of excitons by the threading dislocation defects [24,25]. The suppression of localized potentials will result in the increase of the probability of the capture of excitons by the defects and therefore shorten τ_{nr}. As a result, the improvement of IQE by the large enhancement in τ_r is compromised by the faster τ_{nr}.

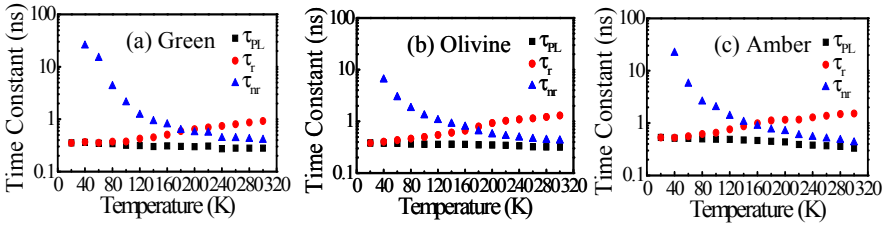

Fig. 4. The radiative and nonradiative lifetime versus temperature derived from measured PL lifetime and IQE for green (a), olivine (b), and amber (c) nanopyramid LED, respectively.

The three substrates were fabricated into 300 μm x 300 μm LED chips using standard LED fabrication steps. Figures 5(a)-5(c) shows the optical microscope images of these LEDs under electrical injection along with the measured light-current-voltage (L-I-V) curves. The dark pats are the p- and n-metal contacts. The I-V curves show typical diode turn on behavior around 3 volts. The turn-on threshold becomes less distinct as the sample changes from G- to A-LED. Above turn-on, the voltage increases significantly up to 6 volts at 200 mA. This is

#191394 - $15.00 USD Received 29 May 2013; revised 23 Aug 2013; accepted 12 Sep 2013; published 23 Sep 2013

higher than the normal c-plane LED driving voltage, indicating a higher serial resistance. It is attributed to the imperfection in the current spreading ITO layer on the corrugated nanopyramid surface. The L-I curves shows a slow turn on of light. It becomes worse in particular for A-LED, where the light does not turn on until the current reaches 40 mA. It implies a considerable current leakage. The leakage paths are likely at the pyramid coalescent boundaries and the apex region, where defects are high. The EL spectra versus injection current are shown in Figs. 5(d)-5(f). The peak emission wavelength blueshifts as the current increases. It is likely related the gradual turn on of the gradient In content MQWs from top to bottom. The blue shifts for G-, O-, and A-LED are about 13, 25, and 50 nm, respectively. The increasing blue shift is due to the increasing polarization field in MQWs as In concentration increases. These blue shift values are, nevertheless, still relatively small compared with that in a c-plane MQW [10,23]. The peak emission wavelengths at 100 mA are 500, 550, and 600 nm, respectively. Their emission colors appear to be green, olivine, and amber, respectively. The slightly redshifted color appearance with respect to their peak emission wavelength is due to the long wavelength tail in the emission spectrum. The full-width-at-half-maximum bandwidths are 60, 80, and 110 nm. The broad spectrum is due to the gradient In distribution in the MQWs. This could be a useful feature in phosphor free white light LED applications if the bandwidth can be further extended.

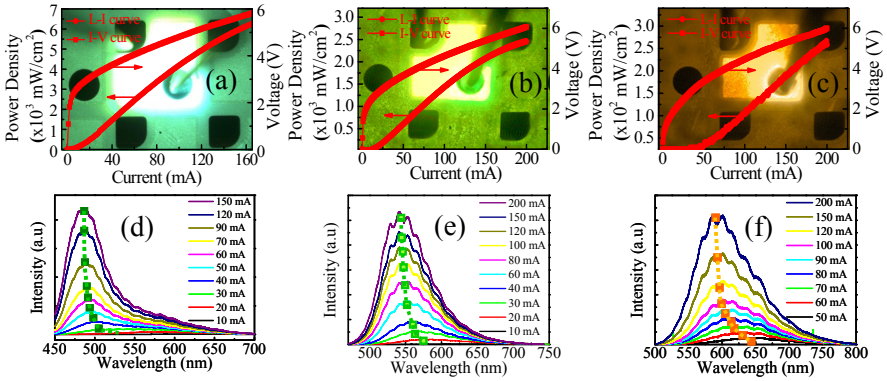

Fig. 5. (a)-(b) Optical microscope images of the G-, O-, and A-LED under electrical injection, showing green, olivine, and amber color. (d)-(f) EL spectrum versus injection current, showing the blue shift of peak emission as current increases due to the screening of polarization field.

4. Conclusion

In summary, we have demonstrated electrically driven green, olivine, and amber color nanopyramid LEDs. MQWs are grown on the nanopyramid semipolar facets. Temperature dependent PL measurement shows high IQEs despite the high In content MQWs. The measured fast radiative lifetime indicates improved radiative recombination efficiency due to the low polarization field in semipolar MQWs. Low localized potential was also observed. It leads to reduced non-radiative lifetime, which partly compromises the enhancement of IQE by the fast radiative lifetime. The electrical injection demonstrates the promising potential of using nanopyramid design for high In content LED applications.

Acknowledgment

The authors thank the support of the National Science Council of Taiwan contract NSC 100-2112-M-001-021-MY3. The authors also thank Dr. T. C. Hsu and M. H. Shieh of Epistar Corporation, Dr. Chung-Hsiang Lin of LuxtalTek Corporation, and the Industrial Technology Research Institute (ITRI) Taiwan for their technical support.